

Post-crack capacity of mechanically reinforced glass beams (MRGB)

J.H. Nielsen & J.F. Olesen

Technical University of Denmark, Department of Civil Engineering, Kgs. Lyngby, Denmark

ABSTRACT: Glass has been used in the building envelope for centuries; however, an increasing trend towards utilizing it for load-carrying structures is seen over the last couple of decades. Glass has a very high compressive strength compared to traditionally load-carrying materials used in civil engineering. On the other hand, due to the brittleness of glass, the tensile strength is governed by surface flaws and is therefore low and unreliable. In order to obtain a ductile global behavior of structural elements made of glass, steel reinforcement can be used in a way similar to what is seen for concrete. In spite of the obvious differences between glass and concrete, several analogies can be drawn between reinforced glass and reinforced concrete. During the last couple of years research in the reinforcement of float glass beams has been carried out, and a ductile behavior has been demonstrated experimentally. The present work is concerned with deriving and verifying design formulas for such beams and investigating the influence on the behavior for different parameters. The design formulas cover the un-cracked state as well as the cracked state and anchorage failure in the form of de-bonding of the reinforcement. The derived formulas are compared with experimental observations and FEM models in order to demonstrate their validity.

1 INTRODUCTION

Glass is used increasingly for structural purposes due to its transparency and high environmental resistance compared to more common structural materials such as concrete and steel. Unfortunately, ordinary glass has a low and unreliable tensile strength due to brittleness and presence of flaws in the surface. The tensile strength (and its reliability) can be improved considerably by tempering the glass; however, this process does not improve the brittleness of the material. Ductility in structural members made of glass has to be obtained by the design of the structural member, similar to what is done for reinforced concrete.

A design providing a ductile behavior can be obtained by gluing a steel band to the bottom (tensile) face of a glass beam (see Figure 1). The yielding of the steel provides the ductility, similar to what is known for reinforced concrete. This concept for a Mechanically Reinforced Glass Beam (MRGB) has been experimentally verified both at Delft University of Technology and the Technical University of Denmark, see e.g. Bos et al. (2004), Louter et al. (2005), Nielsen & Olesen (2007) and Ølgaard et al. (2009).

The external forces on the glass beam are transferred to the reinforcement by (almost) pure shear in the adhesive layer. The properties of the adhesive layer are therefore crucial for the overall perform-

ance of the MRGB, especially with respect to the post-crack behavior where we obtain the ductility.

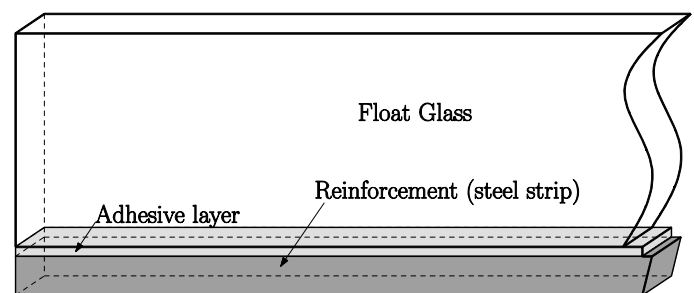


Figure 1. Drawing of a mechanically reinforced glass beam (MRGB) consisting of float glass, adhesive and a steel strip at the bottom of the glass.

1.1 Failure modes

There are four possible failure modes of MRGB, namely: *Anchorage*, *Under-reinforced*, *Normal-reinforced* and *Over-reinforced*.

The *Anchorage* failure is characterized by failure in the adhesive (typically delamination) before yielding of the reinforcement. This type of failure will (most often) occur after cracking of the glass. If the adhesive is strong enough to transfer shear stresses corresponding to a bending moment larger than the glass cracking moment (M_{tg}), a ductile behavior can be achieved; otherwise the failure must be characterized as brittle. A drawing showing the behavior for the anchorage failure can be seen in Figure 2a. It should be noted that in a design situa-

tion it is important to choose a value for M_{tg} which is equal to or lower than the corresponding strength of the glass.

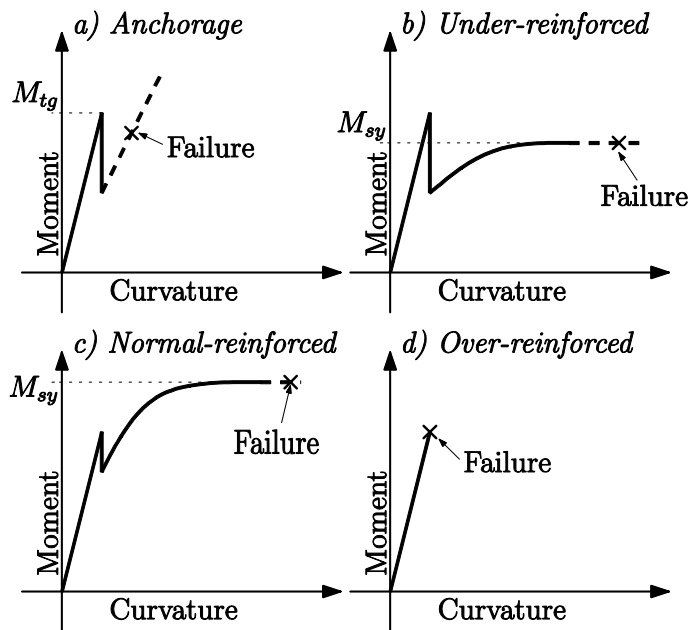


Figure 2. The four different principle behavior for MRGB, assuming a displacement controlled loading.

A principle drawing of the *Under-reinforced* MRGB can be seen in Figure 2b. It is seen that the adhesive is strong enough to prevent anchorage failure, but the yield force in the steel, M_{sy} , is too low compared to M_{tg} . Such a behavior would result in a brittle failure if the loading was force controlled.

The *Normal-reinforced* MRGB is characterized by a yield moment, M_{sy} , which is higher than M_{tg} . This is illustrated in Figure 2c, where extensive deformation capacity along with an increase in the load is seen.

The MRGB is characterized as *Over-reinforced* when the maximum compressive stresses in the glass exceed the compressive strength of the glass, and a brittle failure occurs. This type of failure is most unlikely since the compressive strength of glass is very high ($f_{cg} > 1000\text{MPa}$, see e.g. Alsop et al. 1999) and the shear stresses in the adhesive would exceed the shear capacity and cause anchorage failure instead.

Due to the simple design of such beams, simple and accurate design formulas can be found for the global behavior of the MRGB, however, the criterion for anchorage failure (after cracking of the glass) is more complicated. This paper presents the anchorage criterion by deriving an analytical expression based on simplifying assumptions and modifying this expression according to FE-simulations.

2 DESIGN FORMULAS FOR MRGB

The design formulas given here only consider the cross section in pure bending. Other phenomena such as loss of stability must be considered separately.

The behavior of a MRGB in bending can be subdivided into three stages: 1) the *un-cracked stage*, where no cracks are present in the glass and a perfect composite action between the glass and the reinforcement is assumed. 2) The *cracked stage* where the glass has cracked, but the steel is still assumed to behave linear elastic, and 3) the *yield stage* where the steel is assumed to behave perfectly plastic (without hardening). Finally, the *anchorage* failure is considered separately.

2.1 Un-cracked stage

In the un-cracked stage, the thickness of the adhesive layer is disregarded and a perfect composite action between the glass and the reinforcement is assumed.

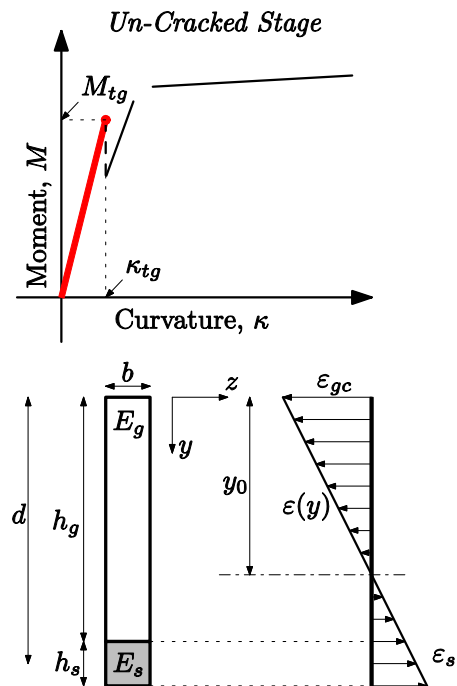


Figure 3. Composite cross-section for the un-cracked stage.

The moment-curvature relation is given by

$$M = \kappa I_t E_g \quad , \quad \kappa \in [0; \kappa_{tg}] \quad (1)$$

where M is the moment, κ is the curvature, E_g is Young's modulus for glass and I_t is the transformed moment of inertia (using E_g for the reference stiffness). The curvature at which the first crack in the glass occurs can be found from the tensile strength of the glass, f_{tg} , by

$$\kappa_{tg} = \frac{f_{tg}}{E_g(h_g - y_0)} \quad (2)$$

where h_g denotes the height of the glass as shown in Figure 3. The depth of the neutral axis is denoted y_0 and can be found from

$$y_0 = \frac{h_g^2 + 2nh_s d}{2(h_g + nh_s)} \quad , \quad n = \frac{E_s}{E_g} \quad (3)$$

where E_s is Young's modulus for the steel and h_s , h_g and d are defined in Figure 3.

These formulas can be used for estimating the moment at which the glass will crack, M_{lg} , which in a design situation defines the upper short-term load limit in the serviceability limit state.

2.2 Cracked stage

The cracked stage is characterized by the glass only transferring compressive stresses which are in equilibrium with the tensile stresses in the reinforcement. Furthermore, this stage is also characterized by a linear elastic material behavior of the reinforcement. The formulas are therefore only valid until initial yielding of the outermost fiber of the reinforcement.

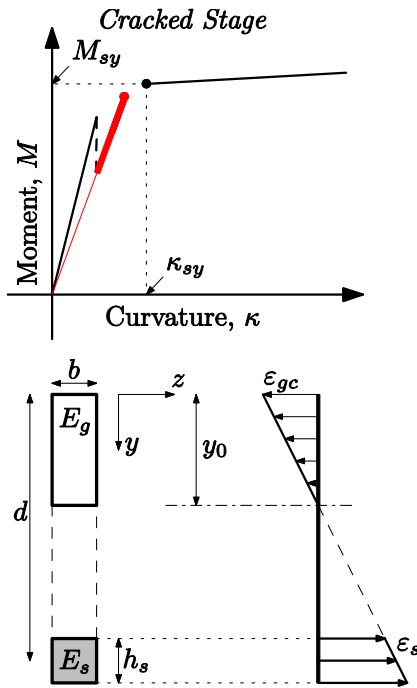


Figure 4. Composite cross-section for the cracked stage without yielding in the steel.

From moment equilibrium (Figure 4) the moment in the cracked stage can be expressed as:

$$M = bh_s E_s \varepsilon_s \left(d - \frac{1}{3} y_0 \right) \quad (4)$$

Utilizing that the curvature can be written as

$$\varepsilon_s = \kappa(d - y_0) \quad , \quad \kappa \in [\kappa_{tg} ; \kappa_{sy}] \quad (5)$$

the moment-curvature relation for the cracked stage can be found as:

$$M = \kappa(d - y_0) bh_s E_s \left(d - \frac{1}{3} y_0 \right) \quad (6)$$

where the depth of the neutral axis can be found from geometric considerations (plane sections remain plane) and force equilibrium:

$$y_0 = nh_s \left(-1 + \sqrt{1 + \frac{2d}{nh_s}} \right) \quad (7)$$

The above equations can be used for estimating initial yielding in the reinforcement by substituting $\varepsilon_s = \varepsilon_{sy} = f_y/E_s$ in (5):

$$\kappa_{sy} = \frac{f_y}{E_s(d - y_0)} \varepsilon_s \quad (8)$$

Substituting, κ_{sy} , in (6) provides a simple estimate of the yield moment, M_{sy} . However, this estimate does not take into account the non-linear stress distribution in the reinforcement and is not able to predict the curvature during yielding of the reinforcement.

2.3 Yield stage

The yield stage is characterized by complete yielding of the reinforcement. The steel is assumed to behave ideally plastic while the glass is cracked and behaves linearly in compression and without tension in the cracked cross-section. It is furthermore assumed that plane sections remain plane.

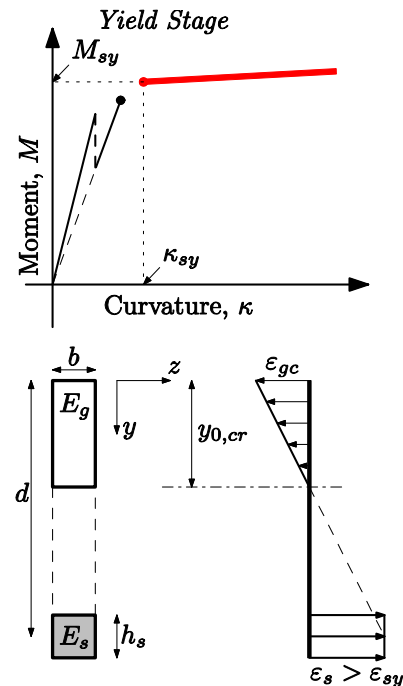


Figure 5. Composite cross-section for the cracked stage with complete yielding of the steel. Ideal plastic behavior of the steel is assumed.

From equilibrium and geometric considerations for the cross-section shown in Figure 5, we can setup the following equation for the maximum compressive strain in the glass.

$$k\varepsilon_{gc}^2 - k\varepsilon_{gc} - k\varepsilon_s = 0, \quad k = \frac{2h_s f_y}{E_g d} \quad (9)$$

Solving this we find (only the positive solution)

$$\varepsilon_{gc} = \frac{h_s f_y}{E_g d} \left(1 + \sqrt{1 + \frac{2E_g d}{f_y h_s} \varepsilon_s} \right) \quad (10)$$

The depth of the neutral axis can be found by geometric considerations and equilibrium:

$$y_0 = \frac{2h_s f_y}{E_g \varepsilon_{gc}} = \frac{d}{\varepsilon_{gc}} k \quad (11)$$

The moment for complete yielding of the steel can be expressed as a function of the strain in the glass:

$$M = bh_s f_y \left(d - \frac{d}{3\varepsilon_{gc}} k \right) \quad (12)$$

The relation between the strain in the glass and the curvature is given by:

$$\varepsilon_{gc} = \kappa y_0, \quad \kappa \geq \kappa_{sy} \quad (13)$$

where it should be noted that y_0 depends on the strain in the steel (or the compressive strain in the glass). This leads to a decrease in y_0 for an increase in the load and therefore the load is slightly increasing even though we assume an ideal plastic behavior of the reinforcement.

2.4 Anchorage failure

As mentioned earlier, the present concept of MRGB relies on the transfer of shear stresses in the adhesive layer between the reinforcement and the glass.

The shear stresses are, as a first approximation, estimated from a simple, modified form of the model for a single lap-joint developed by Volkersen (1938). By comparison with FE-simulations it is shown that this formula is inaccurate and a modification based on the FE study is suggested.

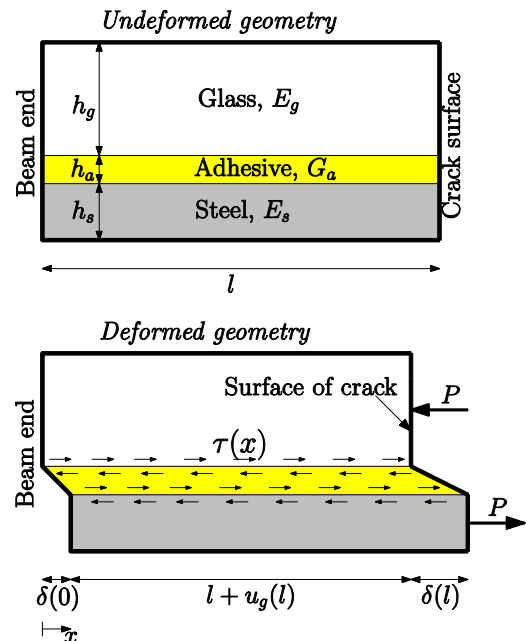


Figure 6. Simplified model. Part of the beam from the crack in the glass to the end of the beam. Axial deformations of the glass and the reinforcement are assumed.

The simplified behavior of the adhesive (and beam) is shown in Figure 6. The shear deformation can be written as

$$\delta(x) = u_s(x) - u_g(x) = \frac{h_a}{G_a} \tau(x) = \delta(0) + \int_0^x \varepsilon_s(x') dx' - \int_0^x \varepsilon_g(x') dx' \quad (14)$$

The normal force in the glass and the steel (per unit thickness) can be expressed by the shear stress as

$$N_g(x) = - \int_0^x \tau(x^*) dx^* = -N_s(x) \quad (15)$$

The normal strains in the glass and the steel can be expressed as:

$$\varepsilon_i(x') = \frac{N_i(x')}{E_i h_i} = \frac{1}{E_i h_i} \int_0^{x'} \tau(x^*) dx^*, \quad i = g, s \quad (16)$$

Substituting (16) into (14), rearranging and differentiating twice we find the following second order homogenous differential equation:

$$\frac{d^2}{dx^2} \tau(x) - \omega^2 \tau = 0, \quad \omega^2 = \frac{G_a}{h_a} \left(\frac{1}{E_g h_g} + \frac{1}{E_s h_s} \right) \quad (17)$$

With the two boundary conditions:

$$N_s(l) = P \quad \wedge \quad u_1(l) + \delta(l) = \delta(0) + u_1(l) \quad (18)$$

where P is the normal force in the steel per unit thickness. The solution of (17) yields

$$\tau(x) = \frac{\omega P}{\sinh(\omega l)} \cosh(\omega x), \quad x \in [0; l] \quad (19)$$

The maximum shear stress is located at the crack (at $x=l$). Furthermore, in the design process it is reasonable only to investigate the anchorage failure corresponding to yielding of the reinforcement, and the following criterion can be derived

$$\frac{\tau_{max}}{f_{\tau,a}} = \frac{\omega f_y h_s \coth(\omega l)}{f_{\tau,a}} < 1 \quad (20)$$

where $f_{\tau,a}$ is the shear strength of the adhesive joint. However, this criterion is too inaccurate and is later modified according to FE calculations in order to provide a simple and realistic criterion for anchorage failure.

3 VERIFICATION OF DESIGN FORMULAS

The theory used for deriving the formulas for the different stages is based on the assumption that plane sections remain plane and the analysis of composite cross-sections and cracked cross-sections, with strong analogies to reinforced concrete. These formulas are compared directly with an experiment for a normal reinforced beam. The design formula for the anchorage failure is compared with a FE-model and modified accordingly.

3.1 Comparison with experimental data

The design formulas for the *un-cracked*, the *cracked* and the *yield* stage can be compared directly with experimentally obtained results.

In Figure 7 the design formulas for the different stages are compared to an experiment for a normal reinforced 1.5m long MRGB in four-point bending, see Nielsen & Olesen (2007). The strength of the glass used was $f_{lg}=28$ MPa which is the mean value estimated from six corresponding glass beams (without reinforcement). The yield stress of the reinforcement was found from experiments to be $f_y=340$ MPa (Nielsen & Olesen (2007)).

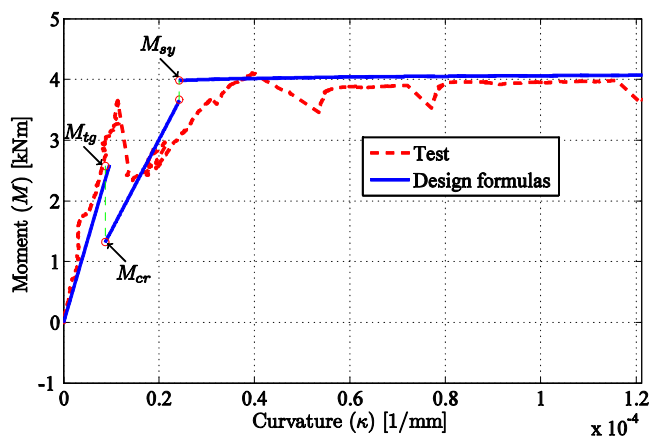


Figure 7. Experimental results compared with the design formulas presented in Section 2.

From Figure 7 it is seen that the design formulas for the three different stages predict the global behavior reasonably well.

3.2 FE-model for the cracked beam

In order to investigate and improve the criterion for anchorage failure (20) a FE model for the cracked stage was set up using the commercial software ABAQUS v6.82. The model only considered a single crack along the symmetry line of the beam as shown in Figure 8.

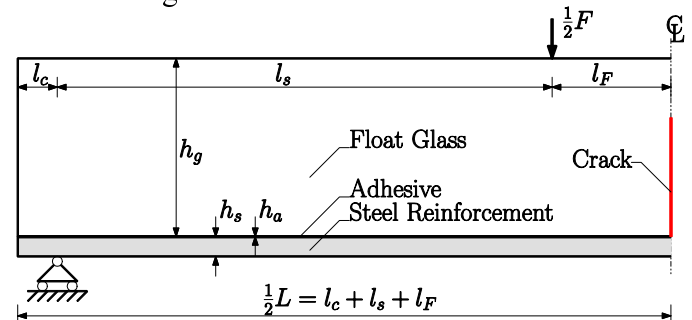


Figure 8. Geometry (symmetric) for the FE-model of the cracked stage. Note the crack in the symmetry line.

Due to the high brittleness of glass, the cohesive forces in the crack can be disregarded. In this single crack model, the fracture of the glass is modeled by not allowing the elements in the glass (at the crack surface) to be in tension. The elements used are LST (linear strain triangle), and a typical mesh (on a deformation plot) for the models is seen in Figure 9. From the figure, it is also seen that the crack is assumed to go through the adhesive as well. However, the response during delamination of the adhesive/steel or adhesive/glass interface is not considered here.

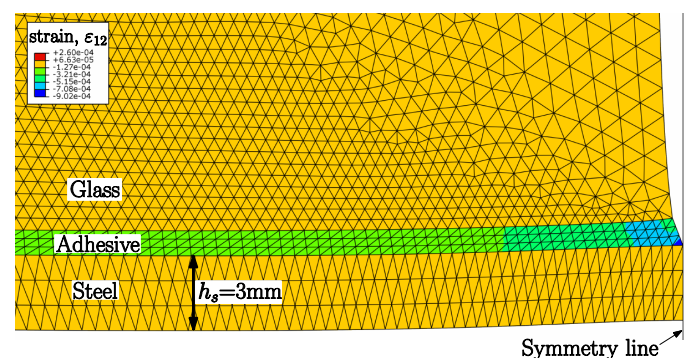


Figure 9. Typical mesh for the FE-model of the single crack. It should be noted that only part of the beam is shown. The parameters for this model are $h_g=150$ mm, $h_a=1$ mm, $h_s=3$ mm, $L=1600$ mm, $G_a=5$ GPa, $M_{max}=10$ kNm, $l_c=50$ mm, $l_f=1$ mm (3-point bending).

Comparing the shear stresses obtained from (20) with the FE-model (Figure 10) it is seen that (20) over estimates the shear stress. Different geometries and shear stiffness for the adhesive has been analyzed by means of the FE-model and compared to the design formula for anchorage failure (20). The

results are summarized in Figure 10 where it is seen that for all investigated geometries (ranging between the two curves enclosing the shaded area) the FE-models have predicted shear stresses lower than the design formula in (20). It is also seen that the ratio between the result of the FE-model and the design formula increases with decreasing shear stiffness of the adhesive.

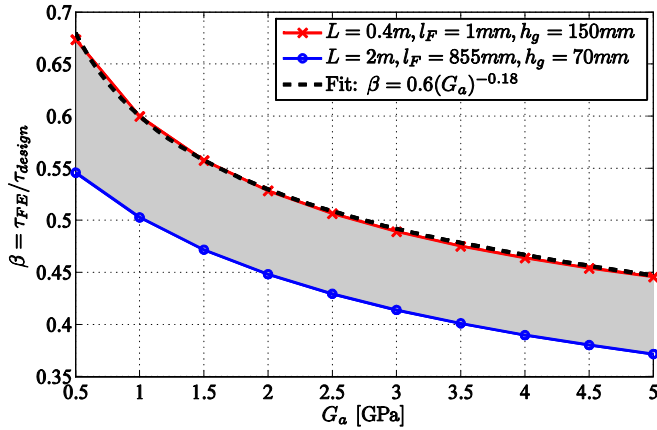


Figure 10. Deviation between the single-crack FE-model and the design formulas given in (20) as a function of the shear modulus of the adhesive. All models investigated use $h_a=1\text{mm}$ and $h_s=3\text{mm}$ as fixed values and variation between the numbers given in the figure.

In Ølgaard et al. (2009) the formula for the anchorage failure is compared with experiments on single-layer (not laminated float glass) MRGB. Here it was found that the predictions by (20) yielded stresses approximately twice the value found at the experiments. Comparing this to Figure 10 the results from the FE-model seem to be reasonable.

From the investigation above, a modified version of (20) can be useful in the design phase of MRGB, where a simple tool is needed. The modified version is given in (21) where the expression in (20) is multiplied by the factor β .

$$\beta \frac{\omega f_y h_s}{f_{\tau,a}} \coth(\omega l) < 1 \quad (21)$$

where the factor β is, conservatively, given by:

$$\beta = 0.6 \left(\frac{G_a}{1\text{GPa}} \right)^{-0.18}, \quad \frac{G_a}{1\text{GPa}} \in [0.5; 5] \quad (22)$$

3.3 Parametric study using the design formulas

The parametric study given here does not cover all parameters; however, it can provide knowledge of some of the most important properties.

In Figure 11 a plot shows the moments and adhesive shear stress (calculated from (21)) as a function of the yield force in the reinforcement. From the figure it is seen that a yield force below 28 kN yields an under-reinforced failure (see Figure 2). On the

other hand, an increasing yield force also increases the shear stress in the adhesive and from the figure it is seen that anchorage failure is predicted for a yield force higher than 60 kN.

It should be emphasized that in the design situation, the moment when the glass breaks, M_{lg} , can be based on a design value (taking into account e.g. the time-dependent strength of the glass) whereas for experiments the actual strength of the glass should be used.

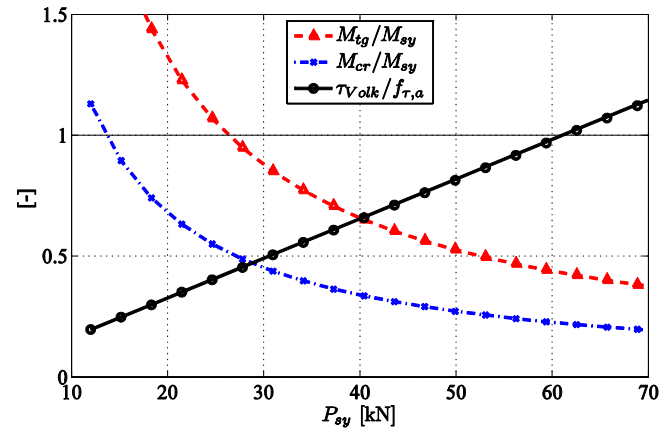


Figure 11. Plot showing the Moments (defined in Figure 7) normalized with the yield moment as a function of the yielding force in the reinforcement. The shear stress in the adhesive found by (21) and normalized with the shear strength of the adhesive.

4 DISCUSSION

This section includes a brief discussion of the design philosophy for the MRGB. Furthermore, an example of the steps in the preliminary design of a MRGB using the formulas provided, is given.

4.1 The effect of time-dependent adhesive layers

In most adhesives, an effect of creep and stress relaxation is present. Figure 12 shows the strain response to a constant loading of an epoxy adhesive.

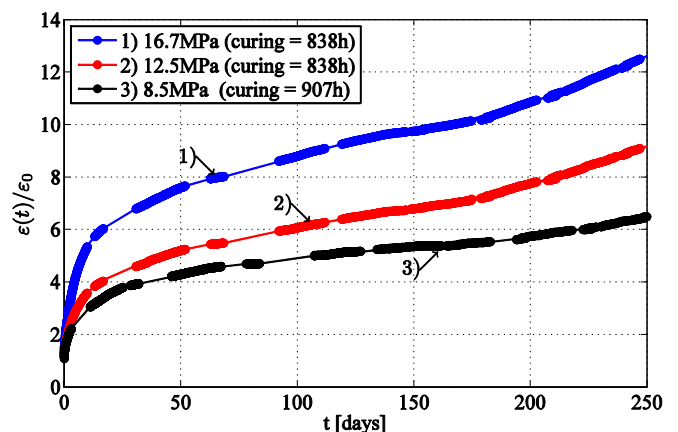


Figure 12. Creep test for an epoxy adhesive. Note that ϵ_0 is the elastic strain corresponding to the strain at $t=0$.

Such behavior complicates the design of MRGB in several aspects. In the un-cracked state the composite action will depend on the duration of loading. Disregarding the bending stiffness of the reinforcement, it will be conservative to assume that the glass is carrying all the long-term loading as shown in Figure 13. Another issue is the relatively low and time-dependent strength of float-glass. To overcome this challenge further research is needed.

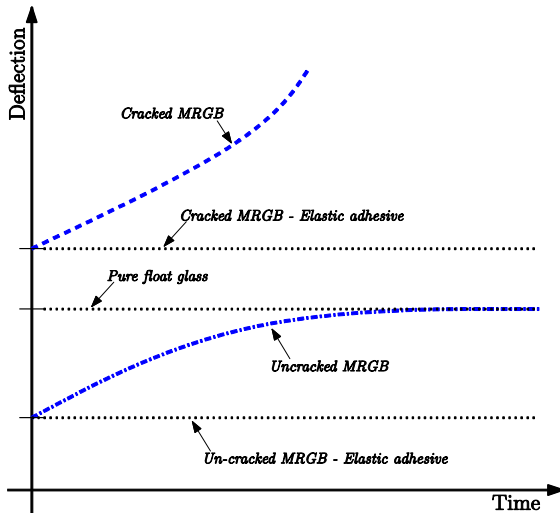


Figure 13. Principle behavior of the deflection for the cracked and un-cracked MRGB (constant loading) using an adhesive with and without time-dependent properties.

Another issue related to the time-dependent behavior of the adhesive concerns the deflections in the cracked stage, where the deflections eventually will increase catastrophically, see Figure 13. It is therefore, necessary to replace the cracked MRGB relatively soon after the appearance of the first crack in the beam. However, if laminated beams are used, the catastrophic development in deflection might be deferred a while. Consequently, laminated glass is preferred over single layer MRGB.

4.2 Example of the use of the design formulas

As an example of the use of the design formulas a 4m long beam loaded with a maximum moment of $M_{max}=4\text{kNm}$ (e.g. a so-called fin in a 4m high facade). The beam is constructed from 2x10mm laminated float glass, and the height of the beam is estimated by assuming the glass to carry the load alone. Assuming the design strength of the glass to be 30 MPa we find the height of the glass to be:

$$h_g = \sqrt{\frac{6M_{max}}{f_{tg}b}} \sim 170\text{mm} \quad (21)$$

As an initial guess; the amount of steel reinforcement is assumed to increase the load capacity in the un-cracked stage with 25%. From a combination of equation (1), (2) and (3), h_s can be found and

in this case it is found to be $h_s \approx 3\text{mm}$. Using a steel with $f_{sy}=420\text{MPa}$ we find a yield force of $P_{sy}=1.26\text{MN/m}$. Using an adhesive layer with the following properties: $G_a=0.9\text{GPa}$, $t_a=1\text{mm}$ and $f_{\tau,a}=32\text{MPa}$ and applying this to (21) along with $E_s=3E_g=210\text{GPa}$, $l=2\text{m}$, $\omega=38.8\text{m}^{-1}$ we find

$$0.61 \frac{38.8\text{m}^{-1} \cdot 1.26\text{MN/m}}{32\text{MN/m}^2} \coth(2 \cdot 38.8) = 0.94 \quad (22)$$

This is less than one, indicating that anchorage failure is not a problem.

5 CONCLUSION

Design formulas for the global behavior of MRGB in bending have been derived. The formulas are covering un-cracked cross-sections, cracked cross-sections and yielding in the reinforcement (for cracked cross sections). Furthermore, a criterion for anchorage failure in the cracked state is developed analytically and modified according to FE-simulations. The set of formulas provided have been compared to experiments and good agreement is shown for the global behavior of the beam.

Even though there exists many analogies between MRGB and reinforced concrete beams, differences exist, especially regarding long term loading. The design philosophy for the MRGB has been discussed in terms of short-term loading versus long-term loading.

REFERENCES

- Bos, F.P., Veer, F.A., Hobbelman, G.J. & Louter, P.C., 2004, Stainless Steel Reinforced and Post-tensioned Glass Beams., *ICEM12 – 12th Int. Conf. on Exp. Mechanics, Politecnico di Bari, Italy, August 29 – September 2 2004.*
- Louter, P.C., Belis, J., Bos, F.P., Veer, F.A. & Hobbelman, G.J., 2005, Reinforced glass Cantilever Beams., *Glass Processing Days, Tampere, Finland, 17-20 June 2005.*
- Nielsen, J.H. & Olesen, J.F., 2007, Mechanically Reinforced Glass Beams. In A. Zingoni (ed.), *Recent Developments in Structural Engineering, Mechanics and Computation; Proc. 3rd intern. Conf., Capetown, 10-12 September 2007.* Rotterdam: Millpress.
- Ølgaard, A.B., Nielsen, J.H. & Olesen, J.F., 2009, *Design of Mechanically Reinforced Glass Beams – Modelling and Experiments*, *Structural Engineering International* 19(2): 130-136.
- Volkersen O., 1938, *Die nietkraftverteilung in zugbeanspruchten nietverbindungen mit konstanten laschenuerschnitten*, *Luftfahrtforschung* 15: 41-47.